

World Journal of *Gastrointestinal Oncology*

World J Gastrointest Oncol 2022 April 15; 14(4): 748-946



REVIEW

- 748 Regulatory RNAs, microRNA, long-non coding RNA and circular RNA roles in colorectal cancer stem cells
Chao HM, Wang TW, Chern E, Hsu SH
- 765 Role of three-dimensional printing and artificial intelligence in the management of hepatocellular carcinoma: Challenges and opportunities
Christou CD, Tsoulfas G
- 794 Role of sirtuins in esophageal cancer: Current status and future prospects
Otsuka R, Hayano K, Matsubara H

MINIREVIEWS

- 808 Vasoactive intestinal peptide secreting tumour: An overview
Una Cidon E
- 820 Management of single pulmonary metastases from colorectal cancer: State of the art
Chiappetta M, Salvatore L, Congedo MT, Bensi M, De Luca V, Petracca Ciavarella L, Camarda F, Evangelista J, Valentini V, Tortora G, Margaritora S, Lococo F
- 833 Current guidelines in the surgical management of hereditary colorectal cancers
Kudchadkar S, Ahmed S, Mukherjee T, Sagar J

ORIGINAL ARTICLE**Basic Study**

- 842 Berberine retarded the growth of gastric cancer xenograft tumors by targeting hepatocyte nuclear factor 4 α
Li LL, Peng Z, Hu Q, Xu LJ, Zou X, Huang DM, Yi P
- 858 Bi-specific T1 positive-contrast-enhanced magnetic resonance imaging molecular probe for hepatocellular carcinoma in an orthotopic mouse model
Ma XH, Chen K, Wang S, Liu SY, Li DF, Mi YT, Wu ZY, Qu CF, Zhao XM
- 872 Xihuang pills induce apoptosis in hepatocellular carcinoma by suppressing phosphoinositide 3-kinase/protein kinase-B/mechanistic target of rapamycin pathway
Teng YJ, Deng Z, Ouyang ZG, Zhou Q, Mei S, Fan XX, Wu YR, Long HP, Fang LY, Yin DL, Zhang BY, Guo YM, Zhu WH, Huang Z, Zheng P, Ning DM, Tian XF

Retrospective Study

- 887 Effect of hepatic artery resection and reconstruction on the prognosis of patients with advanced hilar cholangiocarcinoma
Li YM, Bie ZX, Guo RQ, Li B, Wang CE, Yan F

- 897** Prognostic significance of serum inflammation indices for different tumor infiltrative pattern types of gastric cancer

Wang YF, Yin X, Fang TY, Wang YM, Zhang L, Zhang XH, Zhang DX, Zhang Y, Wang XB, Wang H, Xue YW

- 920** Regorafenib combined with programmed cell death-1 inhibitor against refractory colorectal cancer and the platelet-to-lymphocyte ratio's prediction on effectiveness

Xu YJ, Zhang P, Hu JL, Liang H, Zhu YY, Cui Y, Niu P, Xu M, Liu MY

Clinical Trials Study

- 935** Genome-wide methylation profiling of early colorectal cancer using an Illumina Infinium Methylation EPIC BeadChip

Wu YL, Jiang T, Huang W, Wu XY, Zhang PJ, Tian YP

ABOUT COVER

Editorial Board Member of *World Journal of Gastrointestinal Oncology*, Hanlin L Wang, MD, PhD, Professor, Department of Pathology and Laboratory Medicine, University of California Los Angeles, David Geffen School of Medicine and Ronald Reagan UCLA Medical Center, Los Angeles, CA 90095, United States.
hanlinwang@mednet.ucla.edu

AIMS AND SCOPE

The primary aim of *World Journal of Gastrointestinal Oncology* (*WJGO*, *World J Gastrointest Oncol*) is to provide scholars and readers from various fields of gastrointestinal oncology with a platform to publish high-quality basic and clinical research articles and communicate their research findings online.

WJGO mainly publishes articles reporting research results and findings obtained in the field of gastrointestinal oncology and covering a wide range of topics including liver cell adenoma, gastric neoplasms, appendiceal neoplasms, biliary tract neoplasms, hepatocellular carcinoma, pancreatic carcinoma, cecal neoplasms, colonic neoplasms, colorectal neoplasms, duodenal neoplasms, esophageal neoplasms, gallbladder neoplasms, etc.

INDEXING/ABSTRACTING

The *WJGO* is now indexed in Science Citation Index Expanded (also known as SciSearch®), PubMed, PubMed Central, and Scopus. The 2021 edition of Journal Citation Reports® cites the 2020 impact factor (IF) for *WJGO* as 3.393; IF without journal self cites: 3.333; 5-year IF: 3.519; Journal Citation Indicator: 0.5; Ranking: 163 among 242 journals in oncology; Quartile category: Q3; Ranking: 60 among 92 journals in gastroenterology and hepatology; and Quartile category: Q3. The *WJGO*'s CiteScore for 2020 is 3.3 and Scopus CiteScore rank 2020: Gastroenterology is 70/136.

RESPONSIBLE EDITORS FOR THIS ISSUE

Production Editor: *Ying-Yi Yuan*; Production Department Director: *Xiang Li*; Editorial Office Director: *Ya-Juan Ma*.

NAME OF JOURNAL

World Journal of Gastrointestinal Oncology

ISSN

ISSN 1948-5204 (online)

LAUNCH DATE

February 15, 2009

FREQUENCY

Monthly

EDITORS-IN-CHIEF

Monjur Ahmed, Florin Burada

EDITORIAL BOARD MEMBERS

<https://www.wjgnet.com/1948-5204/editorialboard.htm>

PUBLICATION DATE

April 15, 2022

COPYRIGHT

© 2022 Baishideng Publishing Group Inc

INSTRUCTIONS TO AUTHORS

<https://www.wjgnet.com/bpg/gerinfo/204>

GUIDELINES FOR ETHICS DOCUMENTS

<https://www.wjgnet.com/bpg/GerInfo/287>

GUIDELINES FOR NON-NATIVE SPEAKERS OF ENGLISH

<https://www.wjgnet.com/bpg/gerinfo/240>

PUBLICATION ETHICS

<https://www.wjgnet.com/bpg/GerInfo/288>

PUBLICATION MISCONDUCT

<https://www.wjgnet.com/bpg/gerinfo/208>

ARTICLE PROCESSING CHARGE

<https://www.wjgnet.com/bpg/gerinfo/242>

STEPS FOR SUBMITTING MANUSCRIPTS

<https://www.wjgnet.com/bpg/GerInfo/239>

ONLINE SUBMISSION

<https://www.f6publishing.com>



Basic Study

Bi-specific T1 positive-contrast-enhanced magnetic resonance imaging molecular probe for hepatocellular carcinoma in an orthotopic mouse model

Xiao-Hong Ma, Kun Chen, Shuang Wang, Si-Yun Liu, Deng-Feng Li, Yong-Tao Mi, Zhi-Yuan Wu, Chun-Feng Qu, Xin-Ming Zhao

Specialty type: Oncology

Provenance and peer review:

Invited article; Externally peer reviewed.

Peer-review model: Single blind

Peer-review report's scientific quality classification

Grade A (Excellent): 0
Grade B (Very good): 0
Grade C (Good): 0
Grade D (Fair): 0
Grade E (Poor): 0

P-Reviewer: Muguruma N, Japan

Received: April 28, 2021

Peer-review started: April 28, 2021

First decision: July 14, 2021

Revised: August 31, 2021

Accepted: March 14, 2022

Article in press: March 14, 2022

Published online: April 15, 2022



Xiao-Hong Ma, Shuang Wang, Deng-Feng Li, Yong-Tao Mi, Xin-Ming Zhao, Diagnostic Radiology, National Cancer Center/National Clinical Research Center for Cancer/Cancer Hospital, Chinese Academy of Medical Sciences and Peking Union Medical College, Beijing 100021, China

Kun Chen, Zhi-Yuan Wu, Chun-Feng Qu, State Key Laboratory of Molecular Oncology, National Cancer Center/Cancer Hospital, Chinese Academy of Medical Sciences & Peking Union Medical College, Beijing 100021, China

Si-Yun Liu, GE Healthcare (China), Beijing 100176, China

Corresponding author: Xin-Ming Zhao, MD, Chairman, Professor, Diagnostic Radiology, National Cancer Center/National Clinical Research Center for Cancer/Cancer Hospital, Chinese Academy of Medical Sciences and Peking Union Medical College, No. 17 Panjiayuan Nanli, Chaoyang District, Beijing 100021, China. zhaoxinming@cicams.ac.cn

Abstract

BACKGROUND

Hepatocellular carcinoma (HCC) is the second leading cause of cancer-related mortality. HCC-targeted magnetic resonance imaging (MRI) is an effective noninvasive diagnostic method that involves targeting clinically-related HCC biomarkers, such as alpha-fetoprotein (AFP) or glypican-3 (GPC3), with iron oxide nanoparticles. However, *in vivo* studies of HCC-targeted MRI utilize single-target iron oxide nanoparticles as negative (T2) contrast agents, which might weaken their future clinical applications due to tumor heterogeneity and negative MRI contrast. Ultra-small superparamagnetic iron oxide (USPIO) nanoparticles (approximately 5 nm) are potential optimal positive (T1) contrast agents. We previously verified the efficiency of AFP/GPC3-double-antibody-labeled iron oxide MR molecular probe *in vitro*.

AIM

To validate the effectiveness of a bi-specific probe *in vivo* for enhancing T1-weighted positive contrast to diagnose the early-stage HCC.

METHODS

The single- and double-antibody-conjugated 5-nm USPIO probes, including anti-

AFP-USPIO (UA), anti-GPC3-USPIO (UG), and anti-AFP-USPIO-anti-GPC3 (UAG), were synthesized. T1- and T2-weighted MRI were performed on day 10 after establishment of the orthotopic HCC mouse model. Following intravenous injection of U, UA, UG, and UAG probes, T1- and T2-weighted images were obtained at 12, 12, and 32 h post-injection. At the end of scanning, mice were euthanized, and a histologic analysis was performed on tumor samples.

RESULTS

T1- and T2-weighted MRI showed that absolute tumor-to-background ratios in UAG-treated HCC mice peaked at 24 h post-injection, with the T1- and T2-weighted signals increasing by 46.7% and decreasing by 11.1%, respectively, relative to pre-injection levels. Additionally, T1-weighted contrast in the UAG-treated group at 24 h post-injection was enhanced 1.52-, 2.64-, and 4.38-fold compared to those observed for single-targeted anti-GPC3-USPIO, anti-AFP-USPIO, and non-targeted USPIO probes, respectively. Comparison of U-, UA-, UG-, and UAG-treated tumor sections revealed that UAG-treated mice exhibited increased stained regions compared to those observed in UG- or UA-treated mice.

CONCLUSION

The bi-specific T1-positive contrast-enhanced MRI probe (UAG) for HCC demonstrated increased specificity and sensitivity to diagnose early-stage HCC irrespective of tumor size and/or heterogeneity.

Key Words: Hepatocellular carcinoma; Molecular imaging; Magnetic resonance imaging; Positive contrast agent; Alpha-fetoprotein; Glypican-3

©The Author(s) 2022. Published by Baishideng Publishing Group Inc. All rights reserved.

Core Tip: Use of single biomarkers might hinder the detection efficiency of existing hepatocellular carcinoma (HCC) molecular probes due to tumor heterogeneity, while negative (T2) contrast agents could result in inaccurate diagnoses. Therefore, we developed double-antigen-targeting magnetic resonance imaging (MRI) probes for hepatic tumors by conjugating alpha-fetoprotein or glypican-3 antibodies simultaneously to a 5-nm ultra-small superparamagnetic iron oxide (USPIO) and investigated its performance in orthotopic HCC mouse model. The bi-specific T1-positive contrast-enhanced MRI probe for HCC demonstrated increased specificity and sensitivity to diagnose early-stage HCC irrespective of tumor size and/or heterogeneity. Moreover, the *in vivo* enhancement of imaging by the USPIO probes appeared dose-dependent and requires further investigation.

Citation: Ma XH, Chen K, Wang S, Liu SY, Li DF, Mi YT, Wu ZY, Qu CF, Zhao XM. Bi-specific T1 positive-contrast-enhanced magnetic resonance imaging molecular probe for hepatocellular carcinoma in an orthotopic mouse model. *World J Gastrointest Oncol* 2022; 14(4): 858-871

URL: <https://www.wjgnet.com/1948-5204/full/v14/i4/858.htm>

DOI: <https://dx.doi.org/10.4251/wjgo.v14.i4.858>

INTRODUCTION

Hepatocellular carcinoma (HCC) is a human malignancy with a high incidence rate, affecting populations worldwide[1,2]. Non-invasive magnetic resonance imaging (MRI) is one of the most accessible and effective methods for clinical HCC screening, diagnosis, and prognosis. Additionally, MRI represents a comprehensive imaging technique which is uninfluenced by ionized radiation and is capable of both morphological and functional imaging. Multiple MRI techniques have been developed including diffusion-weighted imaging[3], perfusion-weighted imaging[4], iron quantification[5], and contrast-agent-based imaging, which use gadolinium hepatobiliary contrast agents or superparamagnetic iron oxide nanoparticles[6,7] for early-stage HCC identification. Functional MRI is of adequate sensitivity and accuracy to diagnose typical HCC with a tumor diameter > 1 cm; however, it remains challenging to identify benign and malignant tumors < 1 cm or micro-hepatocellular carcinoma (MHCC) due to undetectable changes in blood supply or a lack of specificity from imaging contrast agents[8,9].

Molecular MRI has led to the development of new strategies to enhance specificity and contrast for early detection of small cancerous tumors[10-12]. The latter has been used by binding early-stage cancer biomarkers with superparamagnetic iron nanoparticles in order to enable active cancer-cell targeting

[13]. The sensitivity and specificity of this technique is dependent on the expression levels of the target molecules, the magnetic relaxivity of the nanoparticles, and the imaging scheme is unlimited by changes in blood supply. Additionally, the active targeting strategy and use of nanoparticles allow for increased specificity and sensitivity than hepatobiliary contrast agents, which are based on hypointense signals associated with cancer foci against normal hepatic parenchyma and solid benign lesions that uptake the agents differently[14,15].

HCC-targeted MRI systems have demonstrated their preclinical effectiveness *in vitro* and *in vivo*. These methods involve binding HCC biomarkers (antibodies, aptamers, or peptide ligands) to iron oxide nanoparticles in order to target clinical HCC-related overexpressed antigens, such as alpha-fetoprotein (AFP) or glypican-3 (GPC3)[16-20]. AFP is a widely used HCC serum biomarker with a specificity and sensitivity of up to 96% and 65%, respectively, and false-positive and false-negative detection rates of approximately 40%[21]. GPC3 is a promising early HCC tissue biomarker expressed on the cell membrane. The biomarker is highly specific for HCC tumors (84.6%) but rare in normal liver parenchyma or benign lesions[22-24]. There are certain limitations of HCC MRI molecular probes. First, single biomarkers might hinder detection efficiency of existing HCC molecular probes due to tumor heterogeneity. Additionally, iron oxide nanoparticles used in the majority of current HCC imaging studies are utilized as negative (T2) contrast agents, which could result in inaccurate diagnosis[25,26]. However, opportunities to improve these probes also exist.

Nanoparticles exhibit size-dependent magnetic properties. Ultra-small superparamagnetic iron oxide (USPIO) nanoparticles of a small core size (approximately 5 nm) are suggested as optimal positive (T1) contrast agents that enhance T1 and suppress T2 signals induced by reductions in volume of magnetic anisotropy, surface spin disorder, and exposure of iron ions with unpaired electrons[26-30]. Additionally, slow phagocytosis of USPIO nanoparticles by macrophages makes them ideal for liver-tumor MRI[31-33]. However, there have been controversial results concerning the T1-specific effects of targeted USPIO probes *in vivo*, mainly concerning whether probe clustering suppresses T1-related effects[26].

Therefore, in this study, we developed double-antigen-targeting MRI probes for HCC tumors by conjugating the AFP and GPC3 antibodies simultaneously to a 5-nm USPIO probe. Our previous study demonstrated that compared with single-target probes, bi-specific probes enhanced the T2-weighted contrast in Hepa1-6 cells expressing AFP and GPC3[34]. The aim of the present study was to provide an *in vivo* validation of the effectiveness of a bi-specific probe for enhancing T1-weighted positive contrast to overcome tumor-heterogeneity limitations in early-stage HCC diagnosis. To this end, we established an orthotopic HCC mouse model and injected double-antigen-targeting MRI probes to investigate probe specificity, sensitivity, and T1/T2 MRI properties using a 3.0 Tesla clinical MR scanner and histologic analysis, relative to observations using single-antibody-labeled and unlabeled USPIO probes.

MATERIALS AND METHODS

Reagents, antibodies, and animals

N-succinimidyl ester-functionalized 5-nm USPIO probes were purchased from Sigma-Aldrich (747440; St. Louis, MO, United States). The alpha fetoprotein antibodies were obtained from Abcam (rabbit monoclonal, ab213328; mouse monoclonal, ab212325; Cambridge, United Kingdom). GPC3 antibodies were obtained from Abcam (rabbit polyclonal, ab66596) and R&D Systems (mouse monoclonal, MAB2119; Minneapolis, MN, United States). Other chemical agents were purchased from Sigma-Aldrich and of analytical grade.

Male C57BL/6J (C57) mice (8-12 weeks old) were purchased from Vital River Laboratory Animal Technology (Beijing, China). The study protocols (NCC2015A011) were approved by the Animal Care and Use Committee of Cancer Hospital, Chinese Academy of Medical Sciences (CH-CAMS). All the mice were maintained under specific pathogen-free conditions at the Laboratory Animal Services Center of CH-CAMS. The animal protocol was designed to minimize pain or discomfort to the animals. The animals were acclimatized to laboratory conditions (23 °C, 12 h/12 h light/dark, 50% humidity, ad libitum access to food and water) for 2 wk prior to establishment of HCC model.

Preparation and physical characterization of antibody conjugated USPIO probes

The synthesis of single- and double-antibody-conjugated USPIO probes, including anti-AFP-USPIO (UA), anti-GPC3-USPIO (UG), and anti-AFP-USPIO-anti-GPC3 (UAG), was performed according to our previously described protocol[34]. Briefly, 18 mg/mL N-succinimidyl ester-functionalized 5-nm USPIO (abbreviated as U) were reacted separately or simultaneously with AFP (ab212325) and GPC3 (MAB2119) antibodies (400 µg/mL each) in phosphate-buffered solution (pH 7.4) at a final volume of 1 mL with gentle stirring for 3 h at room temperature approximately 23 °C to form the final probes.

The morphology and size distribution of the USPIO core were characterized by transmission electron microscopy (TEM; FEI Tecnai G² F30; FEI, Hillsboro, OR, United States) using an acceleration voltage of 300 kV. The hydrodynamic diameters of the U, UA, UG, and UAG probes were measured by dynamic light scattering (DLS; Zetasizer Nano ZS90, Malvern Instruments, Malvern, United Kingdom) using a

non-invasive back scatter mode with a detected scattering angle of 173° at 25 °C.

USPIO phantom imaging and quantitative analysis

To investigate the MRI characteristics of USPIO, the phantom was constructed using USPIO water solutions with gradient concentrations, which were transferred to individual wells (300 µL) of a 96-well plate (iron concentrations of each USPIO solution: 5, 2, 1.5, 1, 0.75, 0.5, 0.25, 0.1, 0.05, and 0.01 mM).

Phantom MRI was performed using a 3.0 Tesla clinical MR scanner (750W; GE Healthcare, Pittsburgh, PA, United States) with an 8-channel head coil. The T1-relaxation times were measured by IR sequence with a fixed echo time (TE) of 7 ms, repetition time (TR) of 2000 ms, and multiple inversion times (TI; 1800, 1500, 1100, 800, 500, 300, 200, and 100 ms). T2 images were acquired using spin echo (SE) sequence with different TE (10–170 ms). The parameters were set as follows: TR (2000 ms), TE (10, 20, 30, 40, 50, 70, 90, 110, 130, 150, and 170 ms), matrix (256 × 256), field of view (FOV; 20 × 20 mm), slice thickness/separation (3 mm/3.3 mm), and number of excitations (NEX; 2.0).

$$SI = A \times [1 - 2 \times \exp(-TI/T1) + \exp(-TR/T1)] \text{ Eq. (1)}$$

$$SI = A \times \exp(-TE/T2) + C \text{ Eq. (2)}$$

$$(1/T_i)_{w} = (1/T_i)_{wo} + r_i [\text{Fe}], i = 1, 2 \text{ Eq. (3)}$$

During data analysis, the two slices in the center at axial view of MRI images for cylinder samples in the 96-well plate were chosen for further analysis. T1- and T2-relaxation times were analyzed in a voxel-based manner by fitting measured T1-signal intensity versus TI according to Eq. (1) and T2-signal intensity versus TE according to Eq. (2), respectively. The proton relaxivities (r_1 : Longitudinal relaxivity; and r_2 : Transverse relaxivity) were obtained from linear regression according to Eq. (3)[35,36]. $(1/T_i)_w$ and $(1/T_i)_{wo}$ represent water-proton relaxation rates (the inverse values of the T1- and T2-relaxation times) in the presence and absence of USPIO.

In vivo experimental procedure

In vivo experiments were performed as illustrated in Figure 1. First, orthotopic HCC models were established using C57 mice. The tumors were allowed to develop for 9 d after inoculation, and mice were prepared for *in vivo* MRI on day ten. Before each USPIO probe injection, the HCC mice were scanned for pre-injection (0 h; baseline) T1- and T2-weighted image collection. Following intravenous probe injection of U, UA, UG, and UAG, T1- and T2-weighted images were collected at 12, 12, and 32 h post-injection. At the end of scanning, mice were euthanized, and histological analyses were performed on tumor samples.

Orthotopic HCC mouse model

Hepa1-6 murine hepatoma cells were purchased from ATCC (CRL-1830; Manassas, VA, United States). GPC3-expressing Hepa1-6 cells (Hepa1-6/GPC3) were established in our laboratory, as previously reported[37], and maintained using standard protocols on media supplemented with 1 mg/mL G418 (Invitrogen, Carlsbad, CA, United States). Hepa1-6/GPC3 cells at the proliferation phase were then cultured in the absence of G418 overnight to generate orthotopic HCC in 8-week-old C57BL/6J mice with weight of 18–20 g. The mice were anesthetized with tribromoethanol (Avertin) at a dosage of 400 mg/kg body weight *via* intraperitoneal injection. The abdominal cavity below the sternum was opened, and the liver was exposed under sterile conditions. A total of 10^6 Hepa1-6/GPC3 cells in 20 µL RPMI-1640 were injected under the liver capsule using a precise micro-syringe (Becton, Dickinson and Company, New Jersey, United States). The tumors were developed after inoculation and were suitable for *in vivo* MRI on day 10.

In vivo MRI assessment

In vivo MRI studies were performed on the 3.0 Tesla MR device (GE Healthcare) with a 4-channel animal coil. During scanning, the abdominal region of the mouse was placed at the center of the coil, with the liver as the target.

Mice were anesthetized using tribromoethanol (Avertin) at a dosage of 400 mg/kg body weight *via* intraperitoneal injection. The anesthesia normally took effect at 3- to 5-min post-injection and was sustained for approximately 30 to 45 min. The anesthetic was kept on ice during the experiment. Solutions of the U, UA, UG, and UAG probes were transferred into medical-grade physiological saline (0.9% sodium chloride; pH = 7.5) with a final usage volume of 200 µL.

Prior to the USPIO probe injection, 12 HCC model mice were anaesthetized. T1- and T2-weighted imaging was conducted successively on all mice in order to select a minimum of eight with observable or obvious tumors. The eight mice were then divided into four groups, each of which was treated with either of the U, UA, UG, or UAG probes, respectively, prior to further MRI experiments. Pre-injection images were recorded as 0 h data, followed by administration of the U, UA, UG and UAG probe solution *via* tail-vein injection at a dose of 0.8 mg Fe/kg (or 1.6 mg Fe/kg) over 5 s when the mice were awake. Mice underwent *in vivo* MRI at 12, 12, and 32 h post-injection. The U-treated animal group was used as the control for comparison with the UA-, UG-, and UAG-treated groups.

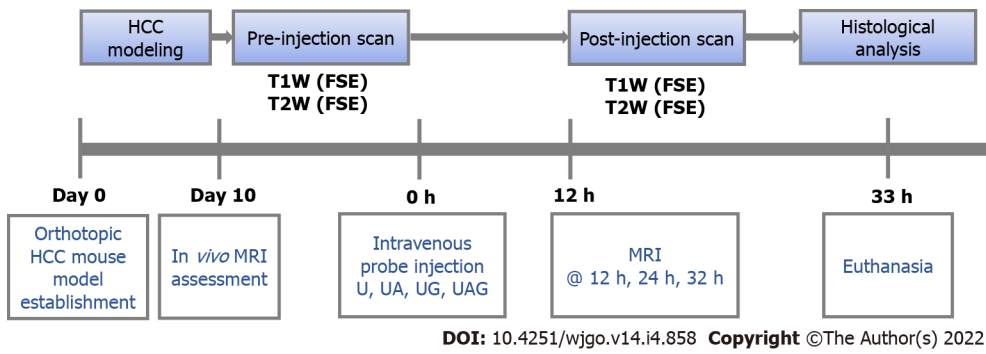


Figure 1 Experiment workflow. Probe treatment and T1- and T2-weighted magnetic resonance imaging were performed on day 10 after establishment of the orthotopic hepatocellular carcinoma mouse model. MRI: Magnetic resonance imaging; HCC: hepatocellular carcinoma; UA: Anti-AFP-USPIO; UG: Anti-GPC3-USPIO; UAG: Anti-AFP-USPIO-anti-GPC3.

Anesthesia was administered at each time point (12, 24, and 32 h) post-injection; however, the subsequent dosage was reduced by 50% compared to the first dosage at 0 h in order to protect the mice and reduce drug resistance.

T1- and T2-weighted images for each USPIO probe were acquired after administering anesthesia using the same MRI sequence used for pre-injection scanning: (1) Axial T1-weighted image/FSE with TR/TE = 475/10 ms, FOV = 60 mm × 60 mm, matrix = 512 × 512, resolution = 0.1172 mm × 0.1172 mm, slice thickness/slice separation = 0.8 mm/1.6 mm, and NEX = 4.0; and (2) Axial T2-weighted image/fast SE with TR/TE = 1500/92 ms, FOV = 60 mm × 60 mm, matrix = 512 × 512, resolution = 0.1172 mm × 0.1172 mm, and slice thickness/slice separation = 0.8 mm/1.6 mm.

T1- and T2-signal enhancement in the tumor respective to the background was analyzed by manually drawing a region of interest (ROI) around the tumor and normal liver parenchyma. To assess tumor intensity, the largest cross section of the tumor was delineated along the outer margin on the T1-weighted or T2-weighted images and the mean intensities were recorded. Considering that the tumor might not be recognized on the T1-weighted images at the pre-injection time point, the tumor was delineated on the pre-injection T2-weighted images and copied to the T1-weighted images for intensity calculation. For liver parenchyma intensity, a ROI with an approximately 3 mm² area on the liver lobes next to the tumor was drawn 2-3 times at different positions. The average of the mean intensity in these ROIs were then taken as the final background liver intensity. Next, the mean intensity of the tumor was divided by the averaged liver background intensity to obtain the tumor-to-background (T/B) ratio. The T/B ratio of mean intensity for the two ROIs was calculated to describe the signal enhancement resulting from each USPIO probe, and the ratio values were averaged for two mice from UAG-, UG-, UA-, and U-treated groups (0.8 mg Fe/kg dosage) respectively if the image quality was acceptable at each time point. The increase of T/B ratios at 12, 24, and 32 h post-injection relative to that at 0 h (pre-injection) were used to describe the binding effect of the probe to the tumor site.

Histologic analysis

Mice were euthanized after MR scanning, and the livers were harvested for histological analysis. Fresh tissues were fixed with 10% paraformaldehyde and embedded in paraffin, after which they were cut into 5-µm thick serial sections. The sections were immunochemically stained according to manufacturer instructions with monoclonal rabbit anti-mouse anti-AFP (ab213328; Abcam) or polyclonal rabbit anti-mouse anti-GPC3 (ab66596; Abcam). Adjacent slices were used for hematoxylin and eosin (H&E) and Prussian Blue staining, respectively. All stained sections were examined under a light microscope at 4 ×, 10 ×, and 20 × magnification. The expression level of AFP or GPC3 and concentrated USPIO were further analyzed by quantifying the ratio of three 3'-diaminobenzidine (DAB-) or Prussian-blue-stained pixels from the tumor region using Image J (Wayne Rasband and contributors, National Institutes of Health, United States. <http://imagej.nih.gov/ij>).

RESULTS

Physical characterization of antibody conjugated USPIO probes

As previously reported[34], the USPIO probes were uniformly dispersed and exhibited a core diameter of 4.88 ± 0.16 nm and an average hydrodynamic diameter of 40.46 ± 0.53 nm. After antibody binding to the USPIO surface, the average hydrodynamic size of UA, UG, and UAG increased to 56.48 ± 0.52 nm, 54.76 ± 1.02 nm, and 59.60 ± 1.87 nm, respectively. The zeta potentials of UA, UG, and UAG were -12.74 mV, -11.22 mV, and -10.23 mV, respectively, varying from the zeta potential of unlabeled USPIO (-26.13 mV).

USPIO phantom MRI and quantitative analysis

The core diameter (4.88 ± 0.16 nm) of USPIO suggests that it has a good potential as a positive contrast agent [26,28,38]. In the present study, we collected the T1- and T2-weighted images of the phantom (Figure 2A and B) and observed positive enhancement (brighter images at higher USPIO concentrations) of the T1-weighted signal and negative enhancement (darker images at higher USPIO concentrations) of the T2-weighted signal according to USPIO concentration. However, the enhancement of the T1-weighted signal was reversed and began decreasing in the absence of iron at a concentration of 0.75 mM.

The T1 and T2 maps calculated for each USPIO concentration were illustrated in Figure 2C. The longitudinal and transversal relaxation times for the T1 and T2 signals, respectively, were calculated from mean values from the T1 and T2 maps for each USPIO concentration. By using the linear fitting, the proton-relaxation rates ($R_1 = 1/T_1$; and $R_2 = 1/T_2$) with respect to the iron ion concentrations according to Eq. (3), we obtained molar relaxivities (r_1 and r_2) of 0.698 ± 0.017 mM⁻¹ s⁻¹ and 41.017 ± 1.484 mM⁻¹ s⁻¹, respectively (Figure 2D and E).

In vivo MRI

T1- and T2-weighted MRIs were performed before and after intravenous injection of the U, UA, UG, and UAG probes into HCC models, respectively (Figures 3 and 4). The T/B ratios of the enhanced T1- and T2-weighted signal intensity enhancement (or increasing rates relative to pre-injection signals) at each time point were calculated and plotted (Figure 5).

We found that the T1- and T2-weighted images showed the tumor site in both dark and bright contrast prior to the administration of each USPIO probe, respectively, which agreed with clinical HCC-diagnosis guidance. For the T1-weighted MRI, we observed a non-homogeneous, brightened signal at HCC foci in mice receiving UAG or UG probes at 24 h post-injection. The T1-weighted T/B signal ratio (TBSR) for UAG-treated mice increased by 46.7% relative to baseline (0 h) and was higher than that of the other probes at approximately 24 h post-injection, which decreased over time. This indicated that the UAG exhibited a higher binding efficiency with the tumor site. UG-treated and UA-treated livers showed a similar trend in signal intensity as those treated with UAG probes, with a 30.7% and 17.7% increase in T1-weighted TBSR at 24 h post-injection relative to baseline, respectively, which was higher than the intensities observed in mice injected with the U probes. However, the intensity contrast trend over time for mice receiving U probes was unclear. It showed a weak signal peak at approximately 12 h post-injection, with a 12.1% increase in intensity relative to pre-injection levels, while some fluctuations also existed after 12 h time point.

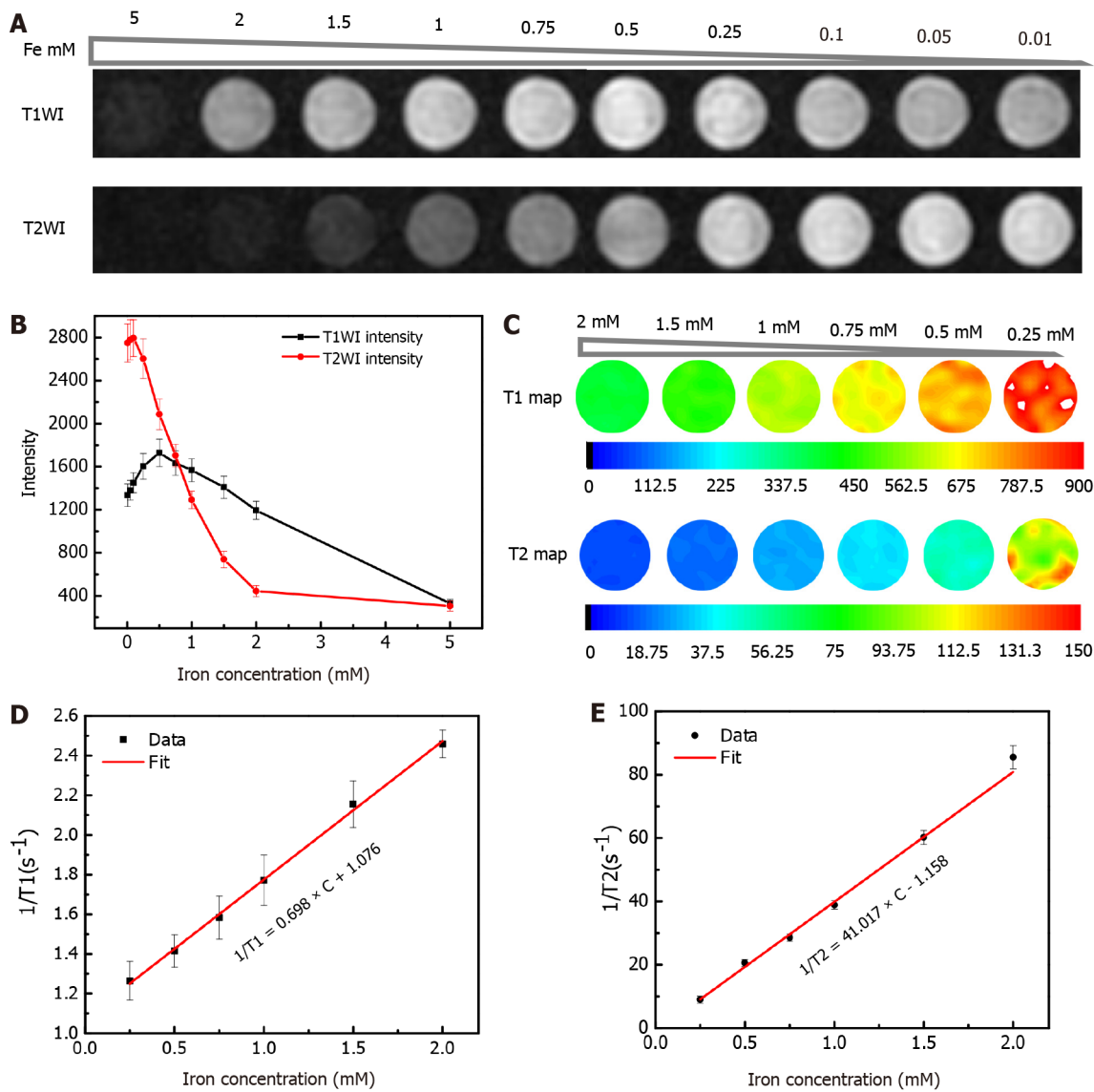
For the T2-weighted MRI, the tumor site showed an initially bright image that darkened after the administration of the targeted USPIO probes. Compared to the pre-injection levels, the TBSR for UAG-treated mice decreased by 11.1% at 24 h post-injection and then increased again over time. Additionally, the ratios in UG- and UA-treated mice increased until 12 h, which subsequently decreased. The ratio in UG-treated mice decreased to its minimum level at 24 h post-injection, with an approximately 1.3% increase in ratio compared with pre-injection. The ratio in UA-treated mice decreased at 24 h post-injection and subsequently decreased by 32.8% at 32 h post-injection with an unknown trend due to measurement suspension. Moreover, the ratio in U-treated mice showed a weak decreasing trend after probe injection until reaching a 9.4% decrease at 24 h compared with pre-injection, which subsequently increased.

Figure 6 illustrated the T1- and T2-weighted images of HCC-mouse livers treated with higher dosages of the UAG probe (1.6 mg Fe/kg body weight), revealing T1-hyperintense and T2-hypointense shrinkage of the tumor at 24 h post-injection of the probes.

Histological analysis

Histological analysis and Prussian Blue staining were used to detect iron uptake and were analyzed qualitatively to evaluate the establishment of the HCC model and *in vivo* MRI results (Figure 7). H&E staining results for U-, UA-, UG-, and UAG-treated livers showed that the tumor cells in the HCC tissues were irregular, with imbalanced nucleus: Cytoplasm ratios and were mostly distributed in lumps. Immunochemical staining verified that the AFP and GPC3 antigens were primarily expressed in the HCC tissue, whereas few were observed in hepatic parenchyma of the same liver.

Uptake of different USPIO probes by the HCC tissue was evaluated by iron Prussian Blue staining (Figure 7). We observed an increase of stained areas distributed in HCC tissues relative to normal liver tissues. A comparison of the U-, UA-, UG-, and UAG-treated tumor sections revealed that UAG-treated mice exhibited a higher accumulation of stained regions relative to those observed in UG- or UA-treated mice. The semi-quantitative results summarized in Supplementary Table 1 might also indicate that UAG-treated mice had higher iron concentrations and targeting specificity in the tumor under similar expression levels for AFP or GPC3. Additionally, all of the targeted USPIO probes exhibited a higher uptake rate for the HCC tissues when compared to the non-targeted USPIO probes. These results indicated that the double-antigen-targeted UAG probe targeted the HCC tissues more effectively than the single-targeted or non-targeted USPIO probes.



DOI: 10.4251/wjgo.v14.i4.858 Copyright ©The Author(s) 2022.

Figure 2 Magnetic resonance imaging properties of ultra-small superparamagnetic iron oxide phantoms. A: T1- and T2-weighted images of a series of 0.9% saline water solutions containing different concentrations of the ultra-small superparamagnetic iron oxide probes as indicated by iron concentration; B: Changes in the T1- and T2-weighted signal intensities according to iron concentration, with standard deviation also illustrated; C: T1 and T2 map illustrated in pseudo color under different iron concentration; D: Linear regression fitting of the longitudinal relaxation-rate ($1/T_1$); E: transversal relaxation-rate ($1/T_2$) data vs different iron concentrations (with standard deviation also illustrated) for extracting the longitudinal relaxivity (r_1) and transverse relaxivity (r_2), respectively.

DISCUSSION

The diagnosis of early-stage HCC is crucial for the establishment of a treatment strategy and for improving prognosis. To this end, molecular probes with high specificity and sensitivity are highly efficacious for HCC imaging. The present study has provided preliminary data supporting the *in vivo* efficacy of USPIO (5-nm core size)-conjugated AFP and GPC3 antibodies for use as a double-antigen-targeted MR molecular probe for HCC. Thereby supporting our hypothesis that it would demonstrate improved targeting efficiency relative to USPIO labeled with a single-antibody or non-targeted USPIOs and functions as a positive contrast agent. We propose that the double-antibody strategy might increase cancer-cell selection and enable tumor-specific diagnosis, regardless of tumor heterogeneity.

We chose the AFP and GPC3 antibodies as biomarkers for HCC targeting. Although several studies demonstrated the feasibility of peptide ligands as biomarkers for binding GPC3[20], we used monoclonal antibodies in the present study to ensure their homogeneity, purity, and avidity.

The histological results demonstrated the preference of the GPC3- and AFP-conjugated USPIO probes (UA, UG, and UAG) for antigen-expressing tumor sites, without any pronounced deposition of the probes in the liver parenchyma. *In vivo* MRI (Figures 3 and 4) provided evidence of the increased tumor-targeting efficiency of the UAG, compared to that observed in single-antibody UG or UA probes, with all of the targeted probes displaying improved specificity than the non-targeted USPIO probe.

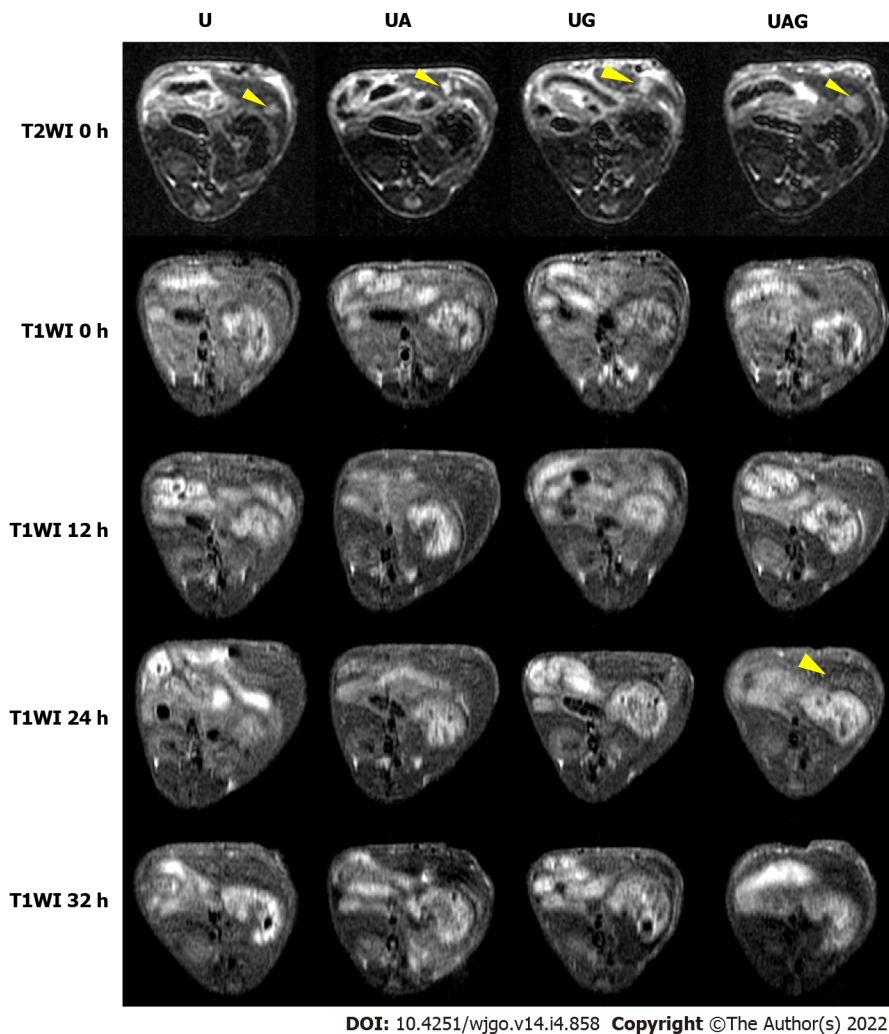
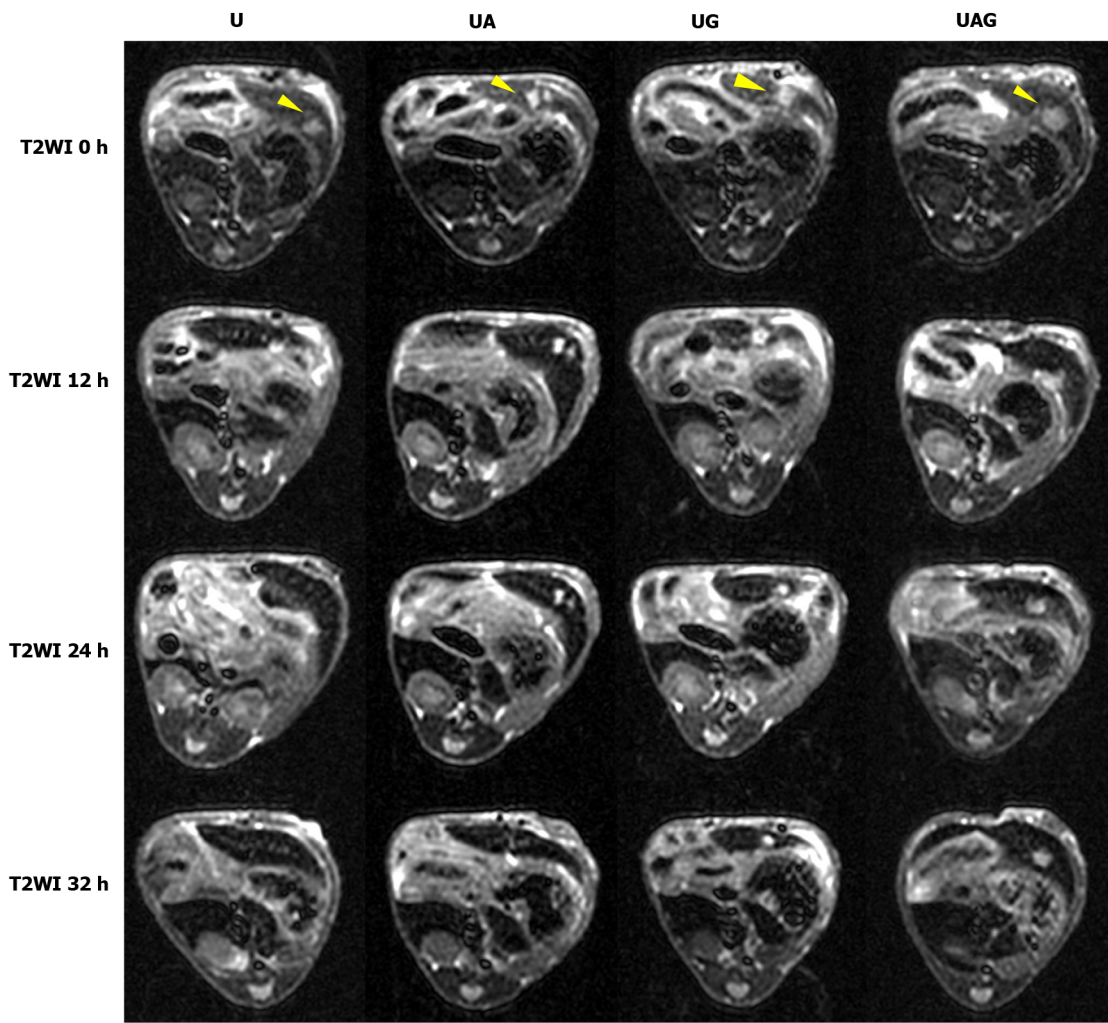


Figure 3 T1-weighted images of hepatocellular carcinoma-model mice administered with ultra-small superparamagnetic iron oxide probes at various time points. Columns represent livers treated with different probes, and the first row shows pre-injection (0 h) T2-weighted images as references for the tumor location indicated by yellow arrowhead. UA: Anti-AFP-USPIO; UG: Anti-GPC3-USPIO; UAG: Anti-AFP-USPIO-anti-GPC3.

Additionally, T1- and T2- weighted MRIs showed that the absolute TBSRs in UAG-treated mice were higher than those in UG-, UA-, and U-treated mice at 24 h post-injection. These results were congruent with those of *in vitro* MRI experiments, showing that UAG-treated Hepa1-6 cells displayed the best T2-weighted contrast[37]. Based on these results, the higher degree of specificity in the binding of UAG to HCC tumors *in vivo* at 24 h post-injection represented the optimal imaging time point for HCC tumors.

Moreover, UG-treated livers showed a similar signal trend to that of UAG-treated livers, with maximal enhancement of the T1-weighted TBSR at 24 h post-injection and higher ratios than that of UA and U probes. This might imply a predominant targeting function by the GPC3 antibody on the part of the UAG probes. Furthermore, the maximum T1-weighted TBSR in UAG-treated mice at 24 h and the 1.24-fold enhancement in the ratio for UA-treated livers compared with U-treated livers at 12 h post-injection might suggest that the AFP antibody was involved in enhancing probe targeting efficiency. However, the signal trend for UA-treated livers was not as significantly distinguishable as those treated with UAG- or UG-, when they were compared with livers signal treated with non-targeted USPIO probes. GPC3 expressed on the cell membrane differed from AFP, which is an antigen secreted into the cytoplasm. We chose AFP as a target based on the tumor site to likely be harboring concentrated amounts of AFP antigens that could be secreted into the serum. Although adding biomarkers for cytoplasmic targeting might help enhance the specificity of double-marker-labeled probes, the optimization of single-target probes specific for cytoplasmic sites might require further consideration.

Iron oxide nanoparticles are widely used for molecular MRI imaging because of their relevant advantages including superparamagnetism, chemical modification, and biosafety[39,40]. The surface modification and hydrodynamic size of iron oxide nanoparticles are essential for optimizing delivery efficiency to their cellular targets[41,42]. Additionally, the core size of the iron oxide nanoparticles significantly influenced their magnetic properties and the MRI effect[27,29,38]. In the present study, N-succinimidyl ester-functionalized USPIO with a core size < 5 nm was purchased and conjugated with AFP and GPC3 antibodies for evaluation as double-antigen-targeting molecular MRI probes for HCC.



DOI: 10.4251/wjgo.v14.i4.858 Copyright ©The Author(s) 2022.

Figure 4 T2-weighted images of hepatocellular carcinoma-model mice administered ultra-small superparamagnetic iron oxide probes at various time points. Columns represent livers treated with different probes. (Yellow arrowhead: tumor location). UA: Anti-AFP-USPIO; UG: Anti-GPC3-USPIO; UAG: Anti-AFP-USPIO-anti-GPC3.

DLS measurements of the U, UA, UG, and UAG probes showed that the hydrodynamic sizes of both double- and single-antibody labeled USPIO probes remained within a range of 50–60 nm. This has the potential to promote applications to determine tumor-vessel permeability and retention effects while avoiding phagocytosis by macrophages rich in normal liver tissue or quick renal clearance[31,41-44]. Moreover, the negative zeta potentials of each of the probes allowed for deeper penetration into tissues [43].

To evaluate the MRI-specific properties of the USPIO probes, we performed both phantom and *in vivo* studies. Phantom results showed that the USPIO probes either positively or negatively enhanced the T1- and T2-weighted signal and shortened the T1- and T2-relaxation times ($r_1 = 0.698 \text{ mM}^{-1} \text{ s}^{-1}$; $r_2 = 41.017 \text{ mM}^{-1} \text{ s}^{-1}$). However, the shortening of r_1 was dose-dependent, and the overdose effect that weakened enhancement of the T1 signal was attributed to the increased T2-relaxation rate observed at higher iron concentrations, which was consistent with previous studies[26]. Therefore, we found that a moderate dosage of 0.8 mg Fe/kg body weight was adequate for the *in vivo* experiments and allowed the determination of T1- and T2-weighted TBSRs for UAG-treated mice at different time points before and after probe injection, up to 24 h post-injection. This differed from a previous report as the aggregation of USPIO probes at the target might have diminished their T1 performance[26]. It is possible that the feasibility of targeted USPIO probes as positive contrast agents is dosage-dependent, as reflected in the T1-hyperintense signal observed at an increased UAG dosage of 1.6 mg Fe/kg body weight (Figure 6). For T2-weighted MRI, only the TBSR in UAG-treated mice showed the best negative enhancement, with an 11.1% decrease until 24 h post-injection relative to the pre-injection TBSR, which was similar to that observed from T1-weighted imaging. The other probes, (UA, UG, and U) did not show significant T2 enhancement or showed a relatively weaker enhancement compared with UAG-treated samples during the first 24 h after probe injection. This might suggest that the double-conjugated antibodies on the UAG probe helped accelerate target recognition during circulation and competed with signal decreases

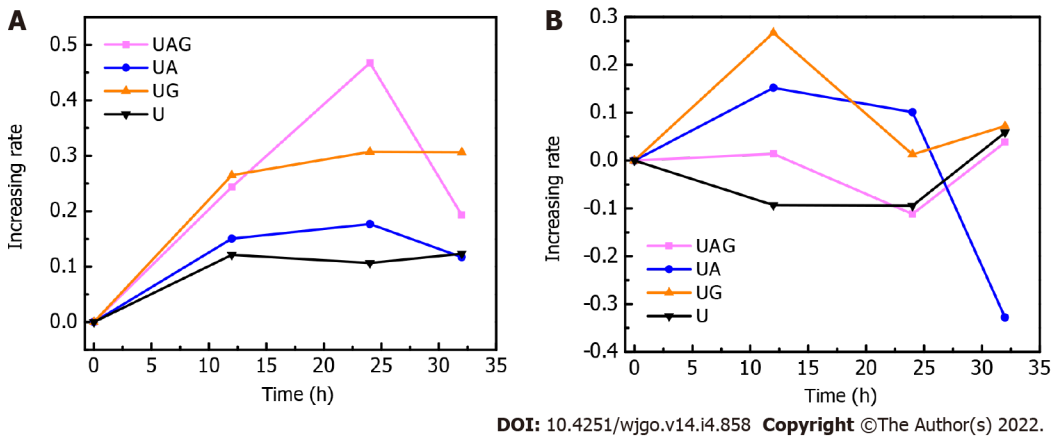


Figure 5 Time-dependent increasing rates of T1- and T2-weighted T/B signal ratios. Increasing rates of T1- and T2-weighted T/B signal ratio at different time points (12, 24, and 32 h) post-injection as compared with pre-injection (0 h) of the U, anti-alpha-fetoprotein (AFP)-ultra-small superparamagnetic iron oxide (USPIO), anti-glypican-3 (GPC3)-USPIO, and anti-AFP-USPIO-anti-GPC3 probes. Data points represent averaged rates from two mice if the image quality was acceptable. A: T1-weighted T/B signal ratios; B: T2-weighted T/B signal ratios. UA: Anti-AFP-USPIO; UG: Anti-GPC3-USPIO; UAG: Anti-AFP-USPIO-anti-GPC3.

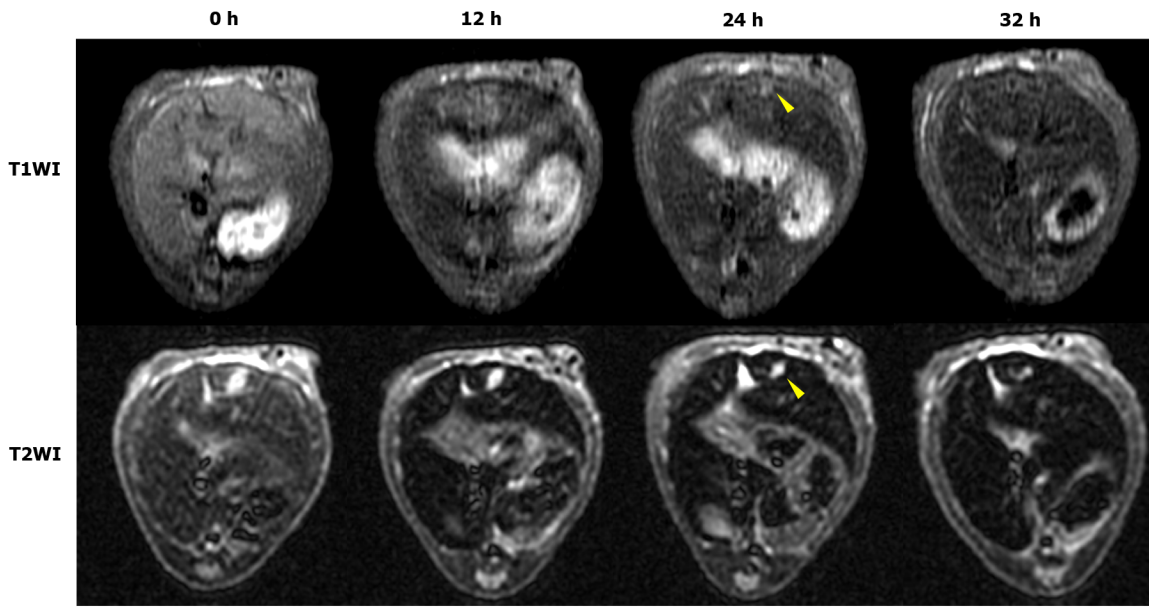
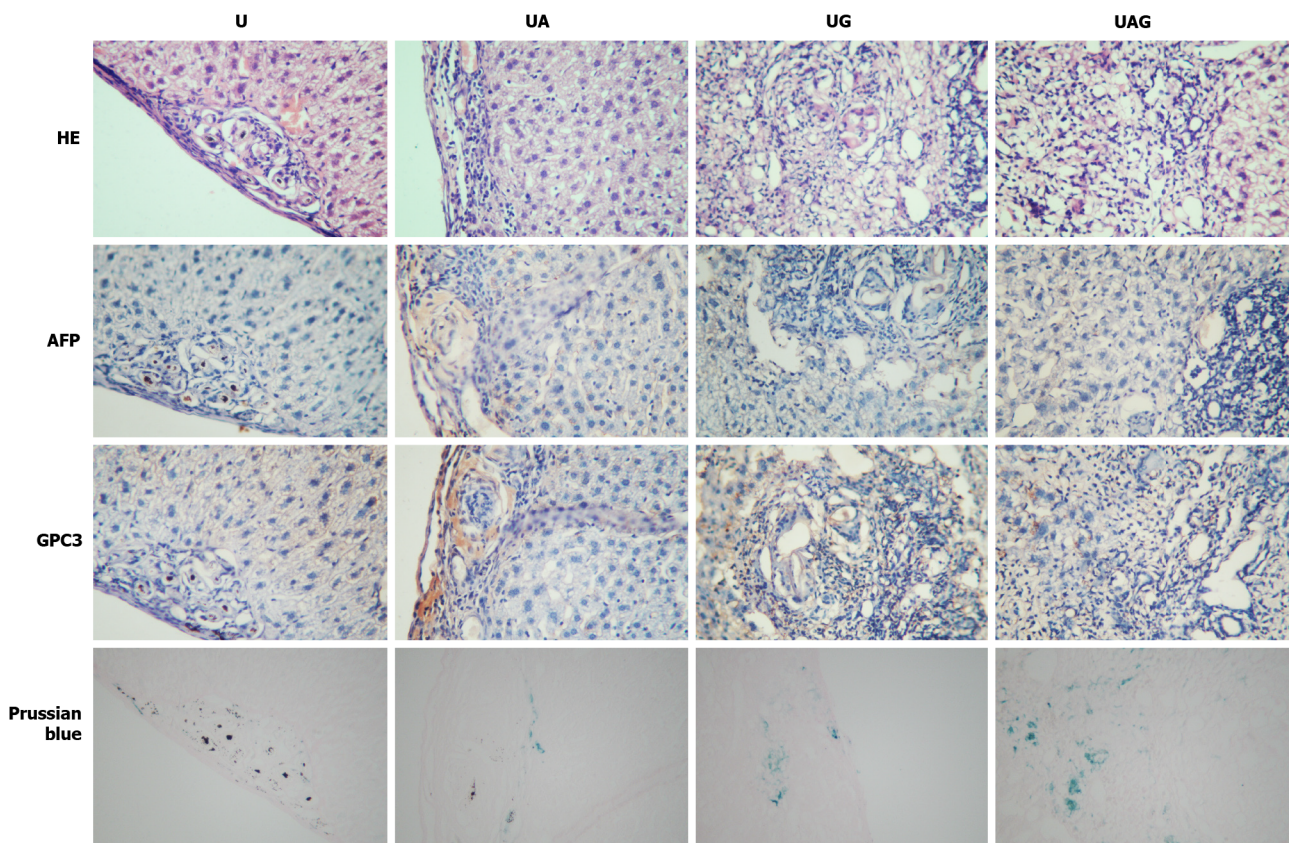


Figure 6 T1- and T2-weighted images of hepatocellular carcinoma-model mice treated with the anti-alpha-fetoprotein-ultra-small superparamagnetic iron oxide-anti-glypican-3 probe (1.6 mg Fe/kg body weight). Top (T1WI) and bottom (T2WI) rows, from left to right: T1- and T2-weighted images, respectively, at 0 h (pre-injection) and 12-, 24-, and 32-h (post-injection). (Yellow arrowhead: Tumor location).

resulting from normal liver uptake.

Clinical hepatobiliary contrast agents primarily bind to organic anion-transporting polypeptides (OATPs) expressed in normal hepatocytes in order to distinguish HCC lesions exhibiting low-level OATP expression. The success of OATP-based agents is highly dependent upon liver function and might lead to confusion for other diseases also exhibiting low-level OATP expression, such as liver metastasis without knowledge of the primary tumor[20,45]. Additionally, the advantages of OATP-based probes are fewer for MHCC exhibiting tumor sizes of < 1 cm[8,20,46]. The double-antibody labeled MRI probes used in the present study allowed for the direct recognition of multiple tumor biomarkers to enhance detection specificity and sensitivity, and has the potential to improve the diagnostic performance for HCC. Specifically, the positive contrast enhancement renders such targeted probes as efficacious for clinical study, although the optimal dosage and imaging time points require further investigation.

This study had several limitations. Firstly, the conjugation of two antibodies might increase the effective molecular weight of the probe and influence its circulation or infiltration rate. We found that the optimal imaging time was approximately 24 h post-injection of the probe, which might be clinically taxing. However, based on the double-labeling strategy described here, it might be possible to utilize



DOI: 10.4251/wjgo.v14.i4.858 Copyright ©The Author(s) 2022.

Figure 7 Histological results of hepatocellular carcinoma tumors treated with U, anti-alpha-fetoprotein-ultra-small superparamagnetic iron oxide, anti-glypican-3-ultra-small superparamagnetic iron oxide, and anti-alpha-fetoprotein-ultra-small superparamagnetic iron oxide-anti-glypican-3 probes. UA: Anti-AFP-USPIO; UG: Anti-GPC3-USPIO; UAG: Anti-AFP-USPIO-anti-GPC3; USPIO: Ultra-small superparamagnetic iron oxide; AFP: Alpha-fetoprotein; GPC3: Glypican-3.

peptides or other ligands with small molecular weights for lesion targeting. Secondly, this study lacked detailed experiments to determine changes in imaging properties according to changes in probe dosage. This preliminary study mainly validated the feasibility of targeted USPIO probes as positive contrast agents; therefore, further dose-related studies are required to explore the unusual T2 effects we observed and to optimize the dosage for improved positive contrast enhancement. Thirdly, the N-succinimidyl ester-functionalized USPIO probe might promote cross-linking with other N-containing molecules, as we observed non-specific binding of the non-targeting USPIO probe with the tumor site. Therefore, a more specific surface modification might be considered in order to optimize the probe design. Lastly, as limited by the experimental conditions, the mice were anesthetized by tribromoethanol (Avertin) *via* intraperitoneal injection, which might increase the difficulty of dosage control among multiple time-point scanning and might limit extended observations with high-imaging quality. In the future studies, gas anesthesia should be adopted to improve the accuracy of dosage control and alleviate potential animal suffering.

CONCLUSION

In this study, we prepared double-antigen-targeting MRI probes for HCC tumors by conjugating AFP and GPC3 antibodies to a USPIO probe < 5 nm in size. *In vitro* phantom experiments revealed that USPIO probes of this size could shorten the longitudinal relaxation time, T1, and transversal relaxation time, T2, making them candidate positive and negative MRI contrast agents. Our *in vivo* MRI results using an orthotopic HCC mouse model demonstrated the efficacy of the UAG probe and its potential for use as a targeted positive contrast agent for HCC based on its increased specificity and sensitivity relative to single-antibody and non-targeted USPIO probes. Moreover, we found that the *in vivo* enhancement of imaging by the USPIO probes was likely dose-dependent and requires further investigation. These findings represent preliminary experimental data to promote the development of optimized molecular MRI systems capable of diagnosing early-stage HCC, regardless of tumor heterogeneity and size.

ARTICLE HIGHLIGHTS

Research background

Hepatocellular carcinoma (HCC) threatened the human heavily. It is urgent to find an effective method to detect and diagnose the HCC early. Our previous study has already verified the efficiency of alpha-fetoprotein (AFP)/glypican-3 (GPC3)-double-antibody-labeled iron oxide magnetic resonance imaging (MRI) molecular probe *in vitro*.

Research motivation

We validated the effectiveness of a bi-specific probe for enhancing T1-weighted positive contrast to detect and diagnose the early-stage HCC in an orthotopic mouse model. It will provide the evidence for the human application.

Research objectives

To *in vivo* validate the effectiveness of a bi-specific probe for early detection and diagnosis of the early-stage HCC.

Research methods

We synthesized the single- and double-antibody-conjugated 5-nm ultra-small superparamagnetic iron oxide (USPIO) probes respectively. T1- and T2-weighted MRI were performed on the mouse model injection of the different probes at 12-, 24-, and 32-h. All the tumor samples were histologically analyzed.

Research results

The bi-specific probe was the most effective kind of the probes in our experiment.

Research conclusions

The bi-specific T1-positive contrast-enhanced MRI probe for HCC demonstrated increased specificity and sensitivity to diagnose early-stage HCC.

Research perspectives

The *in vivo* enhancement in imaging by the USPIO probes was likely dose-dependent and requires further investigation.

FOOTNOTES

Author contributions: Ma XH, Qu CF, and Zhao XM designed the research; Ma XH, Liu SY, Chen K, Wu ZY, Li DF and Mi YT performed the research; Ma XH, Wang S and Liu SY contributed new reagents or analytic tools; Ma XH, Liu SY, and Chen K analyzed the data and wrote the paper.

Supported by PUMC Youth Fund, No. 2017320010; Chinese Academy of Medical Sciences (CAMS) Research Fund, No. ZZ2016B01; and Beijing HopeRun Special Fund of Cancer Foundation of China, No. LC2016B15.

Institutional animal care and use committee statement: This study was approved by the ethics committee of National Cancer Center/Cancer Hospital, Chinese Academy of Medical Sciences and Peking Union Medical College.

Conflict-of-interest statement: The authors declare that there are no conflicts of interest regarding the publication of the paper.

Data sharing statement: No additional data is available.

ARRIVE guidelines statement: The authors have read the ARRIVE guidelines, and the manuscript was prepared and revised according to the ARRIVE guidelines.

Open-Access: This article is an open-access article that was selected by an in-house editor and fully peer-reviewed by external reviewers. It is distributed in accordance with the Creative Commons Attribution NonCommercial (CC BY-NC 4.0) license, which permits others to distribute, remix, adapt, build upon this work non-commercially, and license their derivative works on different terms, provided the original work is properly cited and the use is non-commercial. See: <https://creativecommons.org/licenses/by-nc/4.0/>

Country/Territory of origin: China

ORCID number: Xiao-Hong Ma 0000-0002-9048-8374; Kun Chen 0000-0003-3146-2577; Shuang Wang 0000-0001-9241-

2018; Si-Yun Liu 0000-0001-5611-382X; Deng-Feng Li 0000-0001-5754-3442; Yong-Tao Mi 0000-0002-8071-0621; Zhi-Yuan Wu 0000-0002-8814-0280; Chun-Feng Qu 0000-0001-9973-0887; Xin-Ming Zhao 0000-0001-7286-771X.

S-Editor: Fan JR

L-Editor: A

P-Editor: Yuan YY

REFERENCES

- 1 **Ferlay J**, Soerjomataram I, Dikshit R, Eser S, Mathers C, Rebelo M, Parkin DM, Forman D, Bray F. Cancer incidence and mortality worldwide: sources, methods and major patterns in GLOBOCAN 2012. *Int J Cancer* 2015; **136**: E359-E386 [PMID: 25220842 DOI: 10.1002/ijc.29210]
- 2 **Chen W**, Zheng R, Baade PD, Zhang S, Zeng H, Bray F, Jemal A, Yu XQ, He J. Cancer statistics in China, 2015. *CA Cancer J Clin* 2016; **66**: 115-132 [PMID: 26808342 DOI: 10.3322/caac.21338]
- 3 **Yang D**, She H, Wang X, Yang Z, Wang Z. Diagnostic accuracy of quantitative diffusion parameters in the pathological grading of hepatocellular carcinoma: A meta-analysis. *J Magn Reson Imaging* 2020; **51**: 1581-1593 [PMID: 31654537 DOI: 10.1002/jmri.26963]
- 4 **Semaan S**, Vietti Violi N, Lewis S, Chatterji M, Song C, Besa C, Babb JS, Fiel MI, Schwartz M, Thung S, Sirlin CB, Taouli B. Hepatocellular carcinoma detection in liver cirrhosis: diagnostic performance of contrast-enhanced CT vs. MRI with extracellular contrast vs. gadoxetic acid. *Eur Radiol* 2020; **30**: 1020-1030 [PMID: 31673837 DOI: 10.1007/s00330-019-06458-4]
- 5 **Horvat N**, Monti S, Oliveira BC, Rocha CCT, Giancipoli RG, Mannelli L. State of the art in magnetic resonance imaging of hepatocellular carcinoma. *Radiol Oncol* 2018; **52**: 353-364 [PMID: 30511939 DOI: 10.2478/raon-2018-0044]
- 6 **Vilgrain V**, Van Beers BE, Pastor CM. Insights into the diagnosis of hepatocellular carcinomas with hepatobiliary MRI. *J Hepatol* 2016; **64**: 708-716 [PMID: 26632635 DOI: 10.1016/j.jhep.2015.11.016]
- 7 **Yang S**, Lin J, Lu F, Han Z, Fu C, Gu H. Use of Ultrasmall Superparamagnetic Iron Oxide Enhanced Susceptibility Weighted and Mean Vessel Density Imaging to Monitor Antiangiogenic Effects of Sorafenib on Experimental Hepatocellular Carcinoma. *Contrast Media Mol Imaging* 2017; **2017**: 9265098 [PMID: 29097941 DOI: 10.1155/2017/9265098]
- 8 **Choi MH**, Choi JI, Lee YJ, Park MY, Rha SE, Lall C. MRI of Small Hepatocellular Carcinoma: Typical Features Are Less Frequent Below a Size Cutoff of 1.5 cm. *AJR Am J Roentgenol* 2017; **208**: 544-551 [PMID: 28026208 DOI: 10.2214/AJR.16.16414]
- 9 **Elsayes KM**, Hooker JC, Agrons MM, Kielar AZ, Tang A, Fowler KJ, Chernyak V, Bashir MR, Kono Y, Do RK, Mitchell DG, Kamaya A, Hecht EM, Sirlin CB. 2017 Version of LI-RADS for CT and MR Imaging: An Update. *Radiographics* 2017; **37**: 1994-2017 [PMID: 29131761 DOI: 10.1148/rg.2017170098]
- 10 **Zhang C**, Liu H, Cui Y, Li X, Zhang Z, Zhang Y, Wang D. Molecular magnetic resonance imaging of activated hepatic stellate cells with ultrasmall superparamagnetic iron oxide targeting integrin $\alpha v \beta 3$ for staging liver fibrosis in rat model. *Int J Nanomedicine* 2016; **11**: 1097-1108 [PMID: 27051285 DOI: 10.2147/IJN.S101366]
- 11 **Chen Q**, Shang W, Zeng C, Wang K, Liang X, Chi C, Yang J, Fang C, Tian J. Theranostic imaging of liver cancer using targeted optical/MRI dual-modal probes. *Oncotarget* 2017; **8**: 32741-32751 [PMID: 28416757 DOI: 10.18632/oncotarget.15642]
- 12 **Mu K**, Zhang S, Ai T, Jiang J, Yao Y, Jiang L, Zhou Q, Xiang H, Zhu Y, Yang X, Zhu W. Monoclonal antibody-conjugated superparamagnetic iron oxide nanoparticles for imaging of epidermal growth factor receptor-targeted cells and gliomas. *Mol Imaging* 2015; **14** [PMID: 26044549 DOI: 10.2310/7290.2015.00002]
- 13 **Dulińska-Litewka J**, Łazarczyk A, Hałubiec P, Szafranski O, Karnas K, Karewicz A. Superparamagnetic Iron Oxide Nanoparticles-Current and Prospective Medical Applications. *Materials (Basel)* 2019; **12** [PMID: 30791358 DOI: 10.3390/ma12040617]
- 14 **Huppertz A**. Modern liver MR imaging contrast agents. *Imag Dec MRI* 2010; **11**: 33-37 [DOI: 10.1111/j.1617-0830.2007.00106.x]
- 15 **Leonhardt M**, Keiser M, Oswald S, Kühn J, Jia J, Grube M, Kroemer HK, Siegmund W, Weitschies W. Hepatic uptake of the magnetic resonance imaging contrast agent Gd-EOB-DTPA: role of human organic anion transporters. *Drug Metab Dispos* 2010; **38**: 1024-1028 [PMID: 20406852 DOI: 10.1124/dmd.110.032862]
- 16 **Li Y**, Chen Z, Li F, Wang J, Zhang Z. Preparation and *in vitro* studies of MRI-specific superparamagnetic iron oxide antiGPC3 probe for hepatocellular carcinoma. *Int J Nanomedicine* 2012; **7**: 4593-4611 [PMID: 22956868 DOI: 10.2147/IJN.S32196]
- 17 **Li YW**, Chen ZG, Zhao ZS, Li HL, Wang JC, Zhang ZM. Preparation of magnetic resonance probes using one-pot method for detection of hepatocellular carcinoma. *World J Gastroenterol* 2015; **21**: 4275-4283 [PMID: 25892879 DOI: 10.3748/wjg.v21.i14.4275]
- 18 **Huang KW**, Chieh JJ, Horng HE, Hong CY, Yang HC. Characteristics of magnetic labeling on liver tumors with anti-alpha-fetoprotein-mediated Fe₃O₄ magnetic nanoparticles. *Int J Nanomedicine* 2012; **7**: 2987-2996 [PMID: 22787394 DOI: 10.2147/IJN.S30061]
- 19 **Zhao M**, Liu Z, Dong L, Zhou H, Yang S, Wu W, Lin J. A GPC3-specific aptamer-mediated magnetic resonance probe for hepatocellular carcinoma. *Int J Nanomedicine* 2018; **13**: 4433-4443 [DOI: 10.2147/IJN.S168268]
- 20 **Li W**, Xiao X, Li X, Xu Y, Ma L, Guo L, Yan C, Wu Y. Detecting GPC3-Expressing Hepatocellular Carcinoma with L5 Peptide-Guided Pretargeting Approach: In Vitro and In Vivo MR Imaging Experiments. *Contrast Media Mol Imaging* 2018; **2018**: 9169072 [PMID: 30275801 DOI: 10.1155/2018/9169072]

- 21 **Tsuchiya N**, Sawada Y, Endo I, Saito K, Uemura Y, Nakatsura T. Biomarkers for the early diagnosis of hepatocellular carcinoma. *World J Gastroenterol* 2015; **21**: 10573-10583 [PMID: 26457017 DOI: 10.3748/wjg.v21.i37.10573]
- 22 **Chauhan R**, Lahiri N. Tissue- and Serum-Associated Biomarkers of Hepatocellular Carcinoma. *Biomark Cancer* 2016; **8**: 37-55 [PMID: 27398029 DOI: 10.4137/BIC.S34413]
- 23 **Wu Y**, Liu H, Ding H. GPC-3 in hepatocellular carcinoma: current perspectives. *J Hepatocell Carcinoma* 2016; **3**: 63-67 [PMID: 27878117 DOI: 10.2147/JHC.S116513]
- 24 **Filmus J**, Capurro M. Glypican-3: a marker and a therapeutic target in hepatocellular carcinoma. *FEBS J* 2013; **280**: 2471-2476 [PMID: 23305321 DOI: 10.1111/febs.12126]
- 25 **Na HB**, Lee JH, An K, Park YI, Park M, Lee IS, Nam DH, Kim ST, Kim SH, Kim SW, Lim KH, Kim KS, Kim SO, Hyeon T. Development of a T1 contrast agent for magnetic resonance imaging using MnO nanoparticles. *Angew Chem Int Ed Engl* 2007; **46**: 5397-5401 [PMID: 17357103 DOI: 10.1002/anie.200604775]
- 26 **Liu ZT**, Cai JL, Su H, Yang J, Sun W, Ma Y, Liu S, Zhang C. Feasibility of USPIOs for T1-weighted MR molecular imaging of tumor receptors. *RSC Advances* 2017; **7**: 31671-31681 [DOI: 10.1039/C7RA04903J]
- 27 **Wang G**, Zhang X, Skallberg A, Liu Y, Hu Z, Mei X, Uvdal K. One-step synthesis of water-dispersible ultra-small Fe₃O₄ nanoparticles as contrast agents for T1 and T2 magnetic resonance imaging. *Nanoscale* 2014; **6**: 2953-2963 [PMID: 24480995 DOI: 10.1039/c3nr05550g]
- 28 **Kim BH**, Lee N, Kim H, An K, Park YI, Choi Y, Shin K, Lee Y, Kwon SG, Na HB, Park JG, Ahn TY, Kim YW, Moon WK, Choi SH, Hyeon T. Large-scale synthesis of uniform and extremely small-sized iron oxide nanoparticles for high-resolution T1 magnetic resonance imaging contrast agents. *J Am Chem Soc* 2011; **133**: 12624-12631 [PMID: 21744804 DOI: 10.1021/ja203340u]
- 29 **Huang J**, Wang L, Zhong X, Li Y, Yang L, Mao H. Facile non-hydrothermal synthesis of oligosaccharides coated sub-5 nm magnetic iron oxide nanoparticles with dual MRI contrast enhancement effect. *J Mater Chem B* 2014 [PMID: 25181490 DOI: 10.1039/C4TB00811A]
- 30 **Bao Y**, Sherwood J A, Sun Z. Magnetic iron oxide nanoparticles as T 1 contrast agents for magnetic resonance imaging. *J Mater Chem C* 2018; **6**: 1280-1290 [DOI: 10.1039/C7TC05854C]
- 31 **Daldrup-Link HE**. Ten Things You Might Not Know about Iron Oxide Nanoparticles. *Radiology* 2017; **284**: 616-629 [PMID: 28825888 DOI: 10.1148/radiol.2017162759]
- 32 **Cortajarena AL**, Ortega D, Ocampo SM, Gonzalez-García A, Couleaud P, Miranda R, Belda-Iniesta C, Ayuso-Sacido A. Engineering Iron Oxide Nanoparticles for Clinical Settings. *Nanobiomedicine (Rij)* 2014; **1**: 2 [PMID: 30023013 DOI: 10.5772/58841]
- 33 **Xiao YD**, Paudel R, Liu J, Ma C, Zhang ZS, Zhou SK. MRI contrast agents: Classification and application (Review). *Int J Mol Med* 2016; **38**: 1319-1326 [PMID: 27666161 DOI: 10.3892/ijmm.2016.2744]
- 34 **Ma XH**, Wang S, Liu SY, Chen K, Wu ZY, Li DF, Mi YT, Hu LB, Chen ZW, Zhao XM. Development and *in vitro* study of a bi-specific magnetic resonance imaging molecular probe for hepatocellular carcinoma. *World J Gastroenterol* 2019; **25**: 3030-3043 [PMID: 31293339 DOI: 10.3748/wjg.v25.i24.3030]
- 35 **Song Y**, Kang YJ, Jung H, Kim H, Kang S, Cho H. Lumazine Synthase Protein Nanoparticle-Gd(III)-DOTA Conjugate as a T1 contrast agent for high-field MRI. *Sci Rep* 2015; **5**: 15656 [PMID: 26493381 DOI: 10.1038/srep15656]
- 36 **Zhou Z**, Lu ZR. Gadolinium-based contrast agents for magnetic resonance cancer imaging. *Wiley Interdiscip Rev Nanomed Nanobiotechnol* 2013; **5**: 1-18 [PMID: 23047730 DOI: 10.1002/wnan.1198]
- 37 **Chen K**, Wu Z, Zang M, Wang C, Wang Y, Wang D, Ma Y, Qu C. Immunization with glypican-3 nanovaccine containing TLR7 agonist prevents the development of carcinogen-induced precancerous hepatic lesions to cancer in a murine model. *Am J Transl Res* 2018; **10**: 1736-1749 [PMID: 30018715]
- 38 **Smolensky ED**, Park HY, Zhou Y, Rolla GA, Marjańska M, Botta M, Pierre VC. Scaling Laws at the Nano Size: The Effect of Particle Size and Shape on the Magnetism and Relaxivity of Iron Oxide Nanoparticle Contrast Agents. *J Mater Chem B* 2013; **1**: 2818-2828 [PMID: 23819021 DOI: 10.1039/C3TB00369H]
- 39 **Kandasamy G**, Maity D. Recent advances in superparamagnetic iron oxide nanoparticles (SPIONs) for *in vitro* and *in vivo* cancer nanotheranostics. *Int J Pharm* 2015; **496**: 191-218 [PMID: 26520409 DOI: 10.1016/j.ijpharm.2015.10.058]
- 40 **Gao Z**, Ma T, Zhao E, Docter D, Yang W, Stauber RH, Gao M. Small is Smarter: Nano MRI Contrast Agents - Advantages and Recent Achievements. *Small* 2016; **12**: 556-576 [PMID: 26680328 DOI: 10.1002/smll.201502309]
- 41 **Kievit FM**, Zhang M. Cancer nanotheranostics: improving imaging and therapy by targeted delivery across biological barriers. *Adv Mater* 2011; **23**: H217-H247 [PMID: 21842473 DOI: 10.1002/adma.201102313]
- 42 **Veisich O**, Gunn JW, Zhang M. Design and fabrication of magnetic nanoparticles for targeted drug delivery and imaging. *Adv Drug Deliv Rev* 2010; **62**: 284-304 [PMID: 19909778 DOI: 10.1016/j.addr.2009.11.002]
- 43 **Feng Q**, Liu Y, Huang J, Chen K, Xiao K. Uptake, distribution, clearance, and toxicity of iron oxide nanoparticles with different sizes and coatings. *Sci Rep* 2018; **8**: 2082 [PMID: 29391477 DOI: 10.1038/s41598-018-19628-z]
- 44 **Longmire M**, Choyke PL, Kobayashi H. Clearance properties of nano-sized particles and molecules as imaging agents: considerations and caveats. *Nanomedicine (Lond)* 2008; **3**: 703-717 [PMID: 18817471 DOI: 10.2217/17435889.3.5.703]
- 45 **Vavricka SR**, Jung D, Fried M, Grützner U, Meier PJ, Kullak-Ublick GA. The human organic anion transporting polypeptide 8 (SLCO1B3) gene is transcriptionally repressed by hepatocyte nuclear factor 3beta in hepatocellular carcinoma. *J Hepatol* 2004; **40**: 212-218 [PMID: 14739090 DOI: 10.1016/j.jhep.2003.10.008]
- 46 **Tang Q**, Ma C. Performance of Gd-EOB-DTPA-enhanced MRI for the diagnosis of LI-RADS 4 category hepatocellular carcinoma nodules with different diameters. *Oncol Lett* 2018; **16**: 2725-2731 [PMID: 30008946 DOI: 10.3892/ol.2018.8884]



Published by **Baishideng Publishing Group Inc**
7041 Koll Center Parkway, Suite 160, Pleasanton, CA 94566, USA
Telephone: +1-925-3991568
E-mail: bpgoffice@wjgnet.com
Help Desk: <https://www.f6publishing.com/helpdesk>
<https://www.wjgnet.com>

